iScience, Volume *26*

Supplemental information

Novel enhancers conferring compensatory transcriptional regulation of Nkx2-5 in heart development

Jiejie Zhang, Chen C. Li, Xin Li, Yaxi Liu, Qianhao Wang, Guangyu Zhang, Haiqing Xiong, Aibin He, and Shanshan Ai

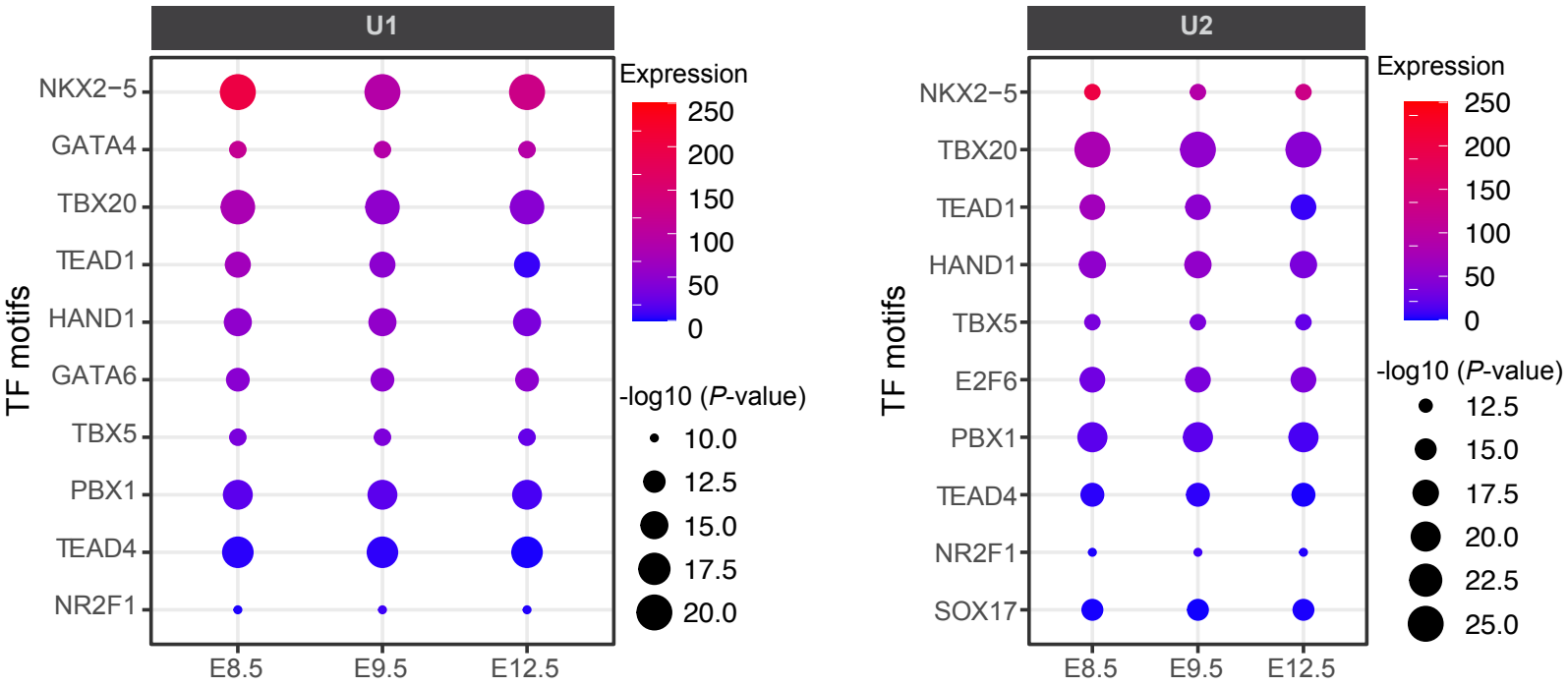

Figure S1. Bubble plots showing the significance of TF motif enrichments in U1 and U2, together with gene expression in different developmental stages, Related to Figure 1.

TF motif analysis was performed by HOMER. P-value was calculated by two-sided binomial test. The top-10 ranked TFs with the highest expression values were shown. The RNA-seq data was downloaded from public database as in Figure 1.

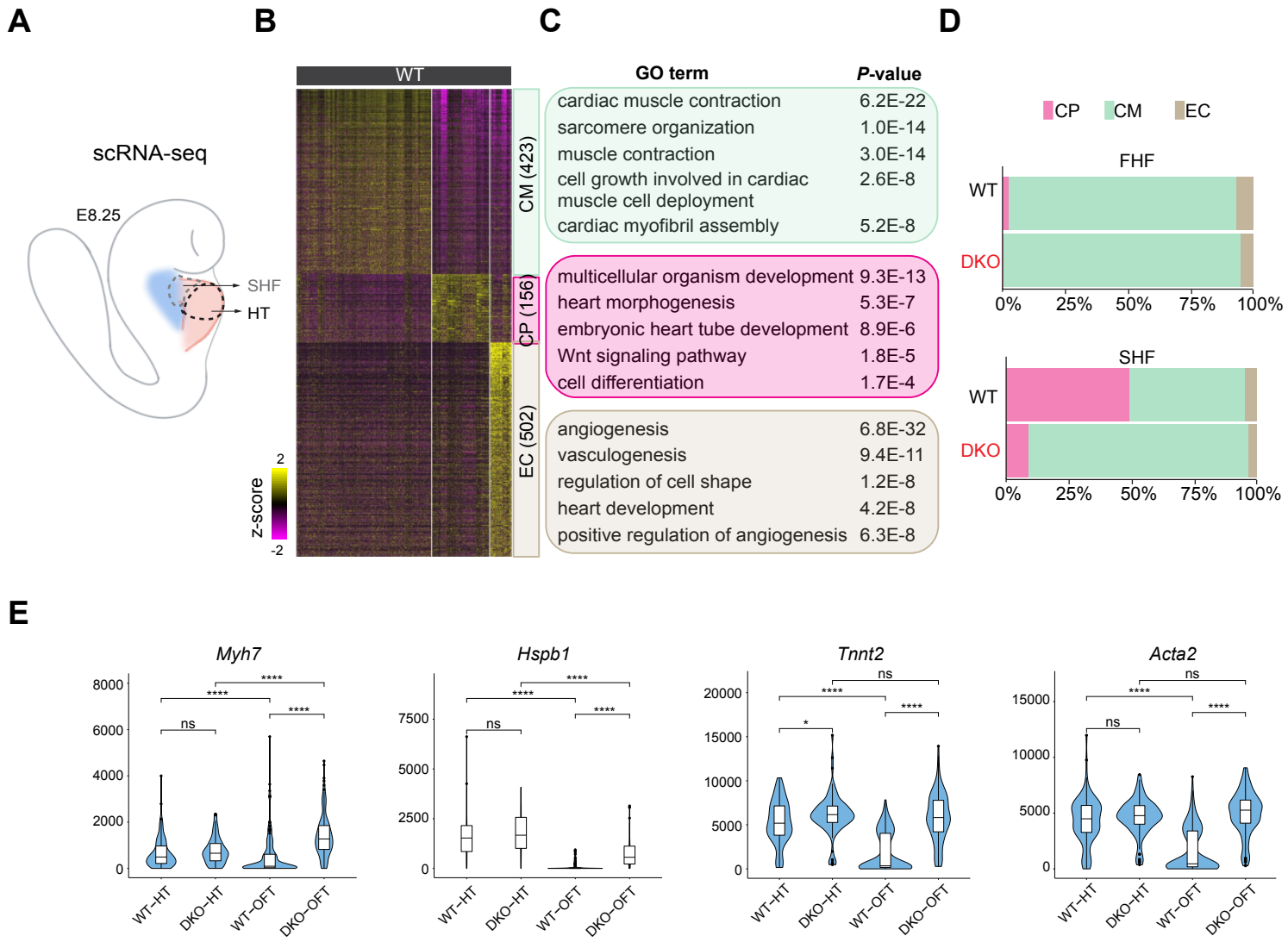

Figure S2. Single-cell RNA-seq analysis reveals precocious differentiation in SHF of E8.25 DKO embryo, Related to Figure 3.

(A) Schematic of separate heart regions microdissected for single-cell dissociation and scRNA-seq. SHF encompasses parts of splanchnic mesoderm and OFT.

(B) Heatmap showing differentially expressed genes (DEGs) in CM, CP and EC populations. The number of DEGs in each cell type was shown on the right.

(C) Top 5 enriched GO terms (Biological Processes) of DEGs for each population as in (B).

(D) Quantification the percentage of CM, CPC and EC in SHF and HT of WT and DKO mouse hearts.

(E) Violin plot showing the expression of cardiomyocyte-specific genes of aggregated single cells from heart tube (HT) and outflow tract (OFT) of E8.25 WT and DKO mice. Statistical significance between 2 groups was determined by the Wilcoxon Rank Sum test (***$P \leq 0.001$). NS indicates not significant.

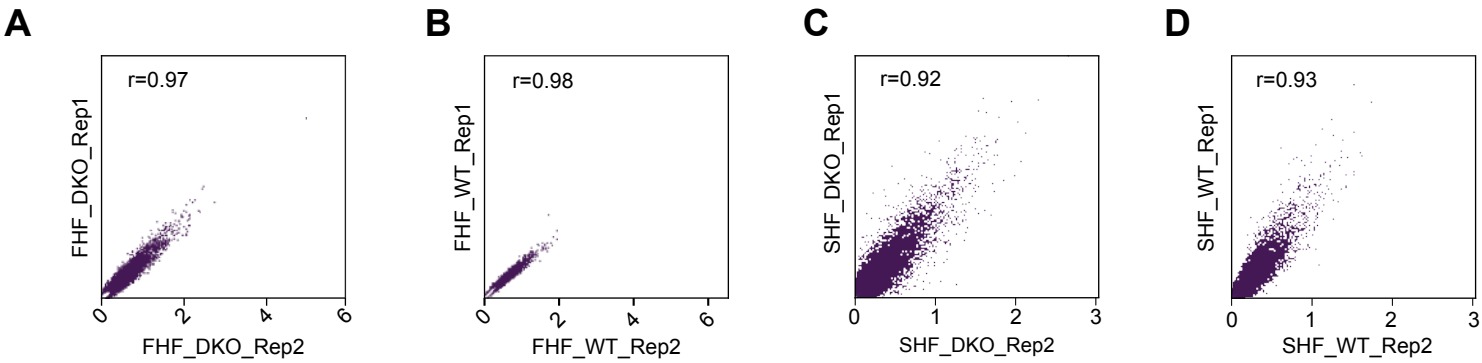

Figure S3. Quality control in H3K27ac ChIP-seq analysis in FHF and SHF of E8.25 WT and DKO hearts, Related to Figure 4. Scatter plots showing the correlation between biological replicates of H3K27ac *in situ* ChIP-seq in FHF (A and B) and SHF (C and D) of E8.25 WT (B and D) and DKO (A and C) hearts.

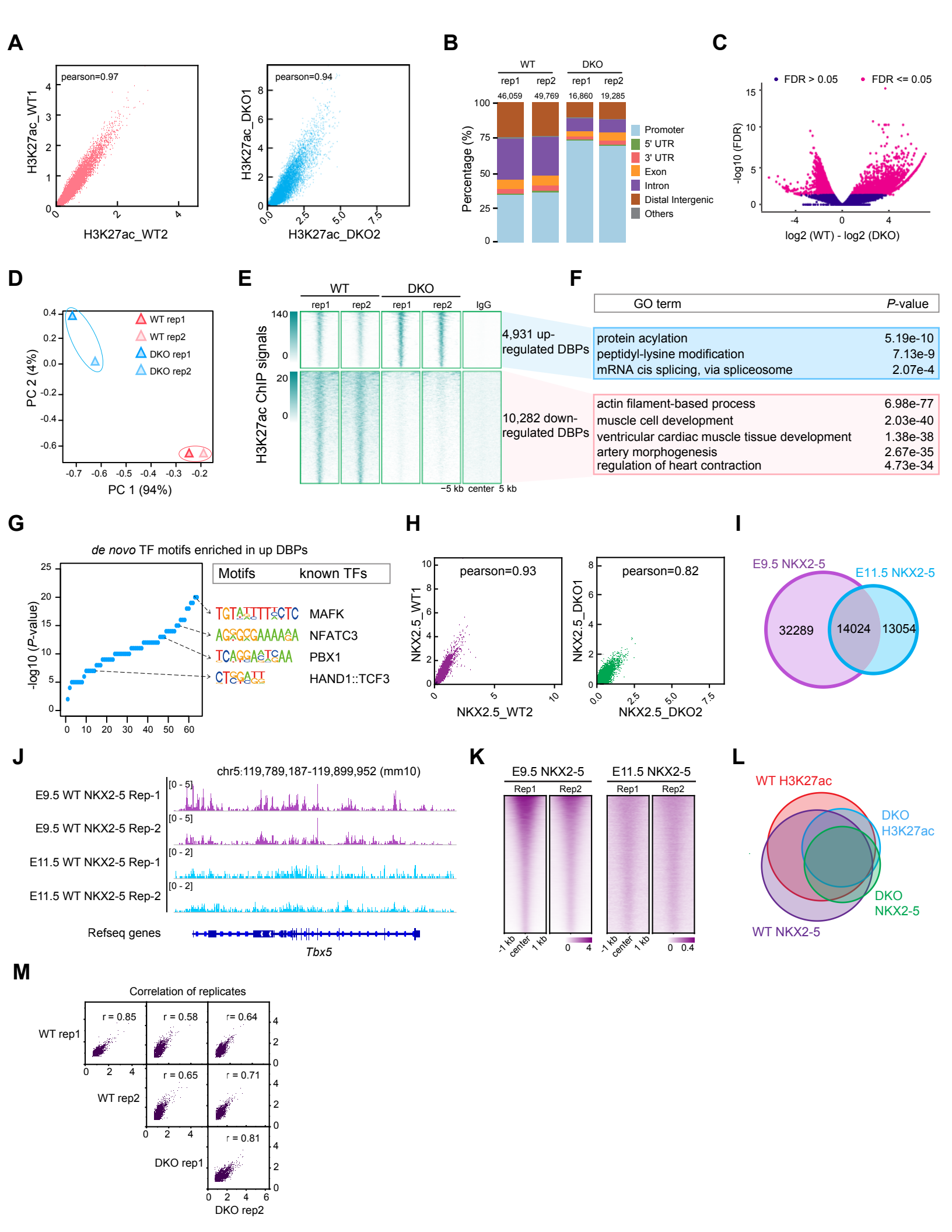
A
pearson=0.97
H3K27ac_WT1
H3K27ac_WT2
pearson=0.94
H3K27ac_DKO1
H3K27ac_DKO2
B
WT
DKO
rep1
rep2
rep1
rep2
46,059
49,769
16,860
19,285
Percentage (%)
Promoter
5' UTR
3' UTR
Exon
Intron
Distal Intergenic
Others
C
FDR > 0.05
FDR <= 0.05
-log10 (FDR)
log2 (WT) - log2 (DKO)
D
WT rep1
WT rep2
DKO rep1
DKO rep2
PC 2 (4%)
PC 1 (94%)
E
WT
DKO
rep1
rep2
rep1
rep2
IgG
H3K27ac ChIP signals
4,931 up-regulated DBPs
10,282 down-regulated DBPs
−5 kb center 5 kb
F
GO term
P-value
protein acylation 5.19e-10
peptidyl-lysine modification 7.13e-9
mRNA cis splicing, via spliceosome 2.07e-4
actin filament-based process 6.98e-77
muscle cell development 2.03e-40
ventricular cardiac muscle tissue development 1.38e-38
artery morphogenesis 2.67e-35
regulation of heart contraction 4.73e-34
G
de novo TF motifs enriched in up DBPs
-log10 (P-value)
Motifs
known TFs
MAFK
NFATC3
PBX1
HAND1::TCF3
H
pearson=0.93
NKX2.5_WT1
NKX2.5_WT2
pearson=0.82
NKX2.5_DKO1
NKX2.5_DKO2
I
E9.5 NKX2-5
E11.5 NKX2-5
32289
14024
13054
J
chr5:119,789,187-119,899,952 (mm10)
E9.5 WT NKX2-5 Rep-1
E9.5 WT NKX2-5 Rep-2
E11.5 WT NKX2-5 Rep-1
E11.5 WT NKX2-5 Rep-2
[0 - 5]
[0 - 5]
[0 - 2]
[0 - 2]
Refseq genes
Tbx5
K
E9.5 NKX2-5
E11.5 NKX2-5
Rep1
Rep2
Rep1
Rep2
-1 kb
center
1 kb
L
WT H3K27ac
DKO H3K27ac
DKO NKX2-5
WT NKX2-5
M
Correlation of replicates
WT rep1
WT rep2
DKO rep1
DKO rep2
r = 0.85
r = 0.58
r= 0.64
r = 0.65
r = 0.71
r = 0.81

Figure S4. ChIP-seq profiling for H3K27ac and NKX2-5 binding in E9.5 WT and DKO hearts, Related to Figure 5.
(A) Scatter plots showing correlation between biological replicates of H3K27ac ChIP-seq data in WT (left) and DKO (right) E9.5 hearts.
(B) Genomic distributions of H3K27ac peaks for DKO and WT ChIP-seq replicates. Values on the top bars indicate peak numbers identified by MACS2 under the same parameters.
(C) Volcano plot showing differential H3K27ac signals in WT versus DKO hearts. Shown in magenta were significantly differential peaks (FDR <= 0.05).
(D) PCA analysis based on 15,213 significantly (FDR <= 0.05) differentially bound peaks (DBPs) across samples.
(E) Heatmaps showing H3K27ac ChIP signals at DBPs. Each column was plotted at the 10 kb regions of the peak center and rows were sorted by signals in Control.
(F) GO terms enriched in genes nearby 4,931 significantly up-regulated DBPs (top) and 10,282 significantly down-regulated DBPs (bottom). *P*-value was calculated by Binomial test.
(G) Dot plots showing *de novo* TF motifs in up-regulated DBPs using Homer. On the right were matched known TFs. *P*-value was calculated by Binomial test.
(H) Scatter plots showing correlation between biological replicates of NKX2-5 ChIP-seq data in WT (left) and DKO (right) E9.5 hearts.
(I) Venn diagram showing overlap of NKX2-5 peaks between E9.5 (this study) and E11.5 (GSE44576) heart.
(J) Track view showing the representative NKX2-5 ChIP signals around the *Tbx5* locus in E9.5 and E11.5 heart as in (I).
(K) Heatmap showing NKX2-5 signals around ±1 kb of 46,880 peaks identified in E9.5 heart.
(L) Venn diagram showing overlap of H3K27ac peaks and NKX2-5 peaks between WT and DKO.
(M) Correlation of contact counts between biological replicates.

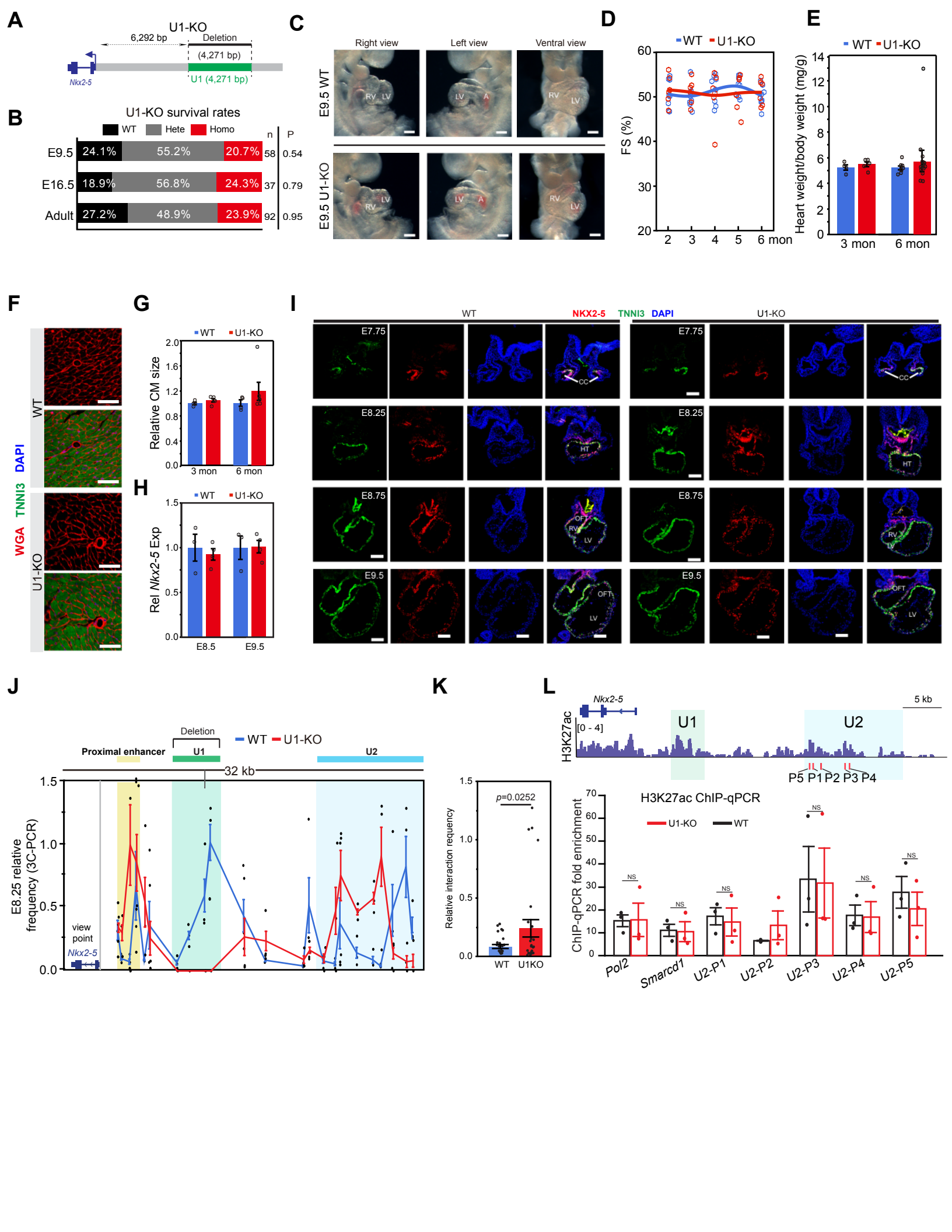
A
U1-KO
6,292 bp
Deletion
(4,271 bp)
Nkx2-5
U1 (4,271 bp)
B
U1-KO survival rates
WT
Hete
Homo
n
P
E9.5
24.1%
55.2%
20.7%
58
0.54
E16.5
18.9%
56.8%
24.3%
37
0.79
Adult
27.2%
48.9%
23.9%
92
0.95
C
Right view
Left view
Ventral view
E9.5 WT
E9.5 U1-KO
RV
LV
A
D
WT
U1-KO
FS (%)
mon
E
WT
U1-KO
Heart weight/body weight (mg/g)
3 mon
6 mon
F
WT
U1-KO
DAPI
TNNI3
WGA
G
WT
U1-KO
Relative CM size
3 mon
6 mon
H
WT
U1-KO
Rel Nkx2-5 Exp
E8.5
E9.5
I
WT
NKX2-5
TNNI3
DAPI
U1-KO
E7.75
E8.25
E8.75
E9.5
CC
HT
OFT
RV
LV
J
Deletion
Proximal enhancer
U1
U2
WT
U1-KO
32 kb
E8.25 relative frequency (3C-PCR)
view point
Nkx2-5
K
p=0.0252
Relative interaction requency
WT
U1KO
L
Nkx2-5
5 kb
H3K27ac
[0 - 4]
U1
U2
P5 P1 P2 P3 P4
H3K27ac ChIP-qPCR
U1-KO
WT
ChIP-qPCR fold enrichment
NS
Pol2
Smarcd1
U2-P1
U2-P2
U2-P3
U2-P4
U2-P5

Figure S5. Characterization of heart morphology and *Nkx2-5* expression of U1-KO mice, Related to Figure 6.

(A) Schematic of the strategy for the U1 knockout (U1-KO) mice generation.

(B) Survival analysis of U1-KO strains determined by heterozygote intercrosses at three indicated developmental stages. *P*-value was calculated by chi-square test.

(C) Gross morphological examination of E9.5 WT and U1-KO mouse hearts. Scale bar, 200 μm. RV, right ventricle; LV, left ventricle; A, atrium.

(D) Heart function measurements by fractional shortening (FS, %) in U1-KO mice and littermate control from 2-month-old to 6-month-old.

(E) Measurement of heart weight/body weight ratio in 3-month-old or 6-month-old WT or U1-KO mice. Data were mean ± s.e.m.

(F) Immunofluorescence staining sections of WGA (wheat germ agglutinin, red), TNNI3 (green) and DAPI (blue) of 3-month-old WT or U1 mice heart. Scale bar, 50 μm.

(G) Quantification of cardiomyocyte (CM) size in 3-month-old or 6-month-old WT or U1-KO mice in immunofluorescence staining sections as in (F). Data were mean ± s.e.m. *P*-value was calculated by Student's t-test.

(H) RT-qPCR of *Nkx2-5* in WT and U1-KO hearts of E8.5 and E9.5 embryos. RNA levels were normalized to 18s rRNA. Data were mean ± s.e.m.

(I) Immunofluorescence staining of NKX2-5 (red), TNNI3 (cardiomyocyte marker, green) and DAPI (blue) in WT and U1-KO hearts at E7.75, E8.25, E8.75, and E9.5. Scale bar, 100 μm; CC, cardiac crescent; HT, heart tube; OFT, outflow tract; RV, right ventricle; LV, left ventricle.

(J) 3C assay results showing interaction frequencies of the *Nkx2-5* TSS with its upstream enhancers in E8.25 wild-type or U1-KO mice. The viewpoint was indicated by the grey bar. The y axis was the interaction frequency relative to that of naked DNA control and normalized data were mean ± s.e.m. (n=3 for each). Yellow shading, proximal enhancer; green shading, U1 enhancer; blue shading, U2 enhancer.

(K) Quantification of the average interaction frequency between *Nkx2-5* promoter and U2 enhancer in (**j**). Data were mean ± s.e.m. *P*-value was calculated by Student's t-test.

(L) H3K27ac ChIP-qPCR showing no significant enrichment around U2 enhancer between E8.25 WT and U1-KO. *Pol2* and *Smarcd1* loci were the positive targets, and U2-P1 to U2-P5 targeted U2 enhancer. Data were mean ± s.e.m. *P*-value was calculated by Student's t-test. NS, not significant.

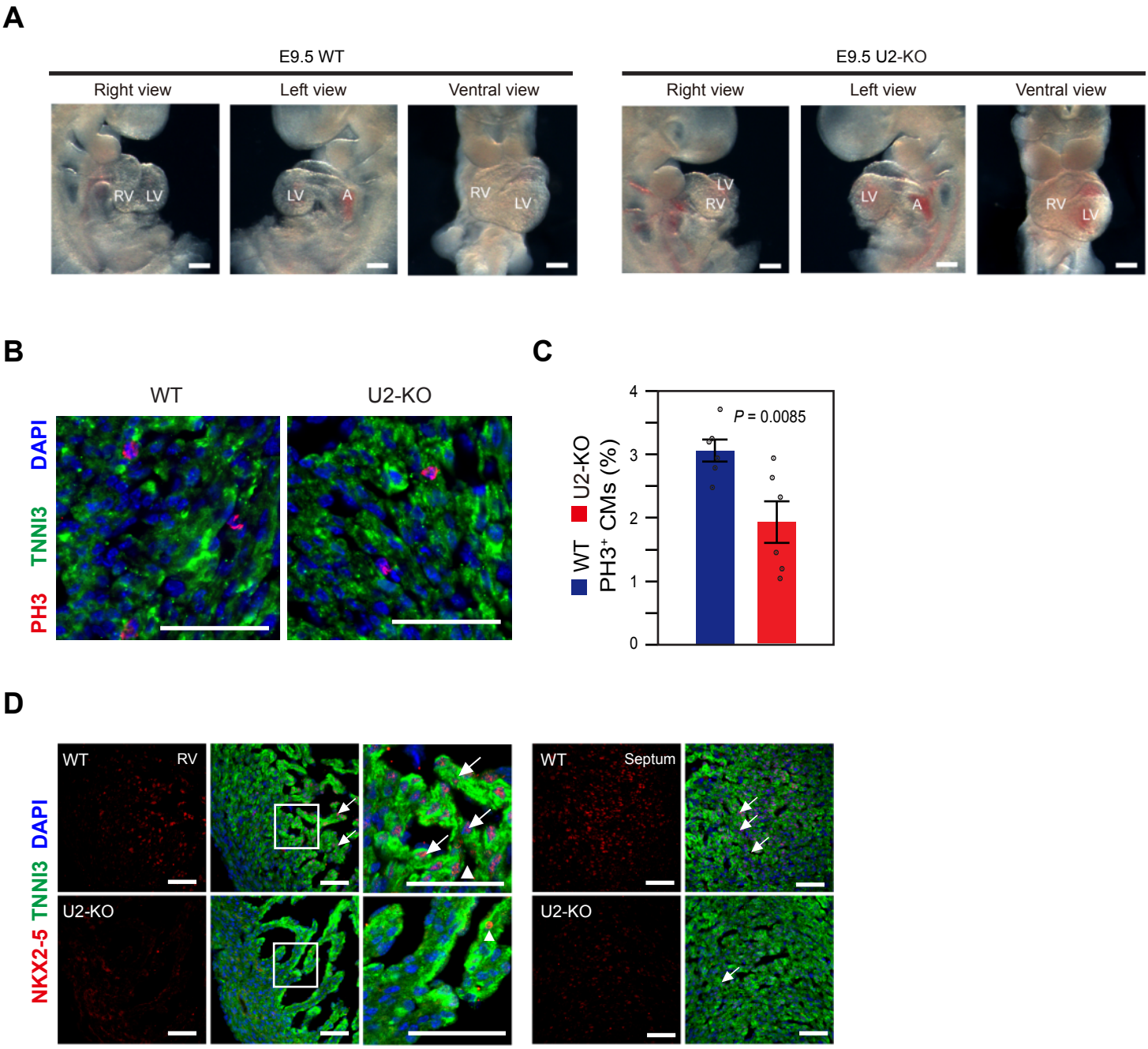

Figure S6. Examination of cardiomyocytes proliferation and *Nkx2-5* expression in U2-KO mouse hearts, Related to Figure 6.

(A) Gross morphological examination of E9.5 WT and U2-KO mouse hearts. Scale bar, 200 μm. RV, right ventricle; LV, left ventricle; A, atrium.

(B) Immunofluorescence staining of PH3 (mitotic marker, red), TNNI3 (green) and DAPI (blue) in WT and U2-KO embryonic hearts at E16.5. Scale bar, 50 μm.

(C) Statistical graph of PH3 positive CMs in WT or U2-KO as in (B). Data were mean ± s.e.m. *P*-value was calculated by Student's t-test.

(D) Immunofluorescence staining of NKX2-5 (red), TNNI3 (green) with DAPI (blue) in WT and U2-KO embryonic hearts at E16.5. Scale bar, 50 μm. Data were mean ± s.e.m. *P*-value was calculated by Student's t-test.

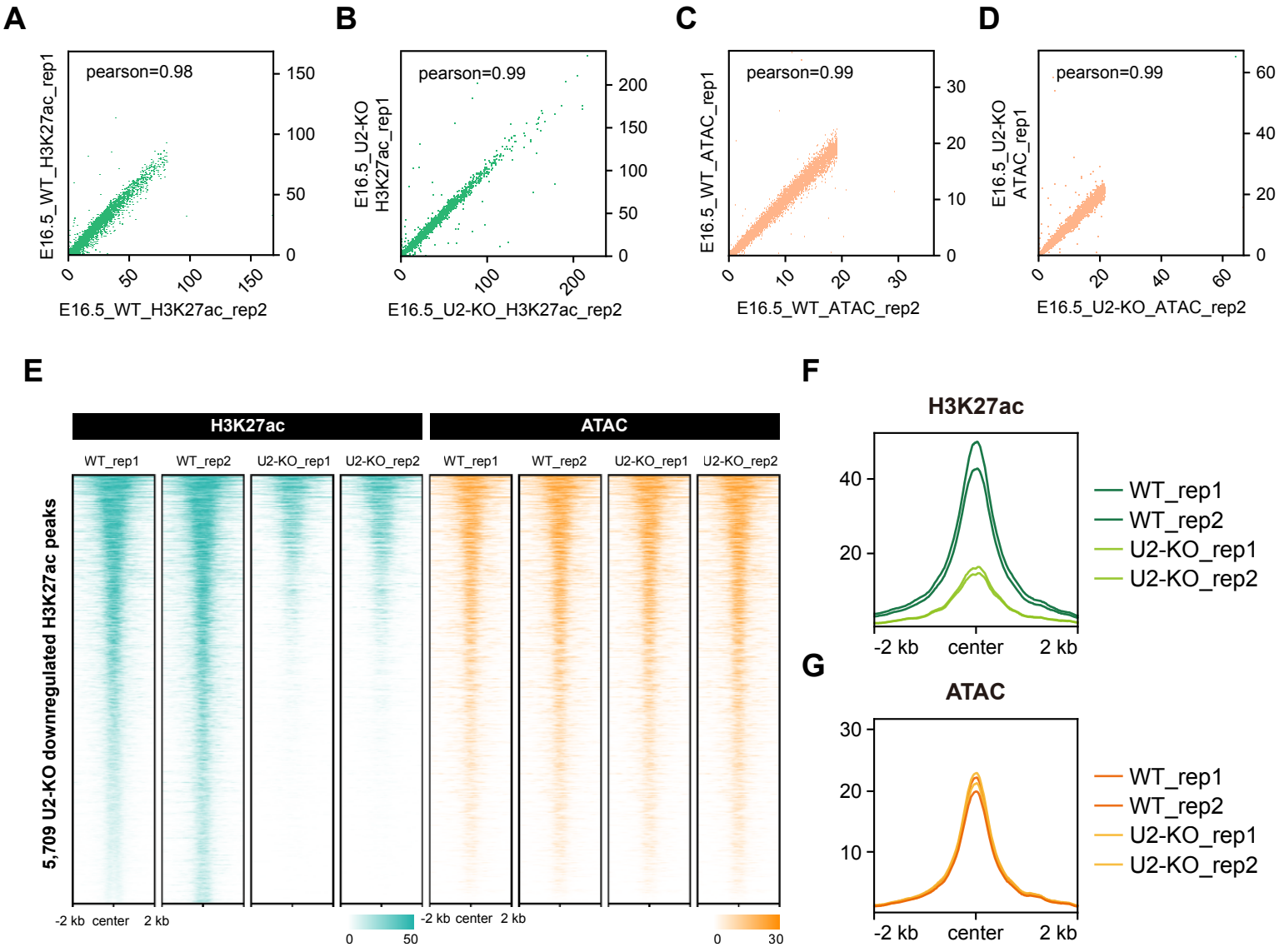

Figure S7. H3K27ac ChIP-seq and ATAC-seq analyses of E16.5 WT and U2-KO hearts, Related to Figure 6.
(A-D) Scatter plots showing the correlation between biological replicates of H3K27ac ChIP-seq (A and B) and ATAC-seq data(C and D) of WT and U2-KO E16.5 mouse hearts.
(E) Heatmap showing H3K27ac ChIP-seq and ATAC-seq signals at 5,709 down-regulated H3K27ac peaks in U2-KO versus WT E16.5 hearts.
(F-G) Aggregate plots of H3K27ac ChIP-seq (F) and ATAC-seq (G) signals at ± 2 kb of 5,709 peak centers in (E).